Index Modulation with PAPR and Beamforming for 5G MIMO-OFDM

Ankur Vora and Kyoung-Don Kang

State University of New York at Binghamton, NY, USA.
{avora4, kang}@binghamton.edu

Abstract— **Although key techniques for next-generation wireless communication have been explored separately, relatively little work has been done to investigate their potential cooperation for performance optimization. To address this problem, we propose a holistic framework for robust 5G communication based on multiple-input-multiple-output (MIMO) orthogonal frequency division multiplexing (OFDM). More specifically, we design a new framework that supports: 1) index modulation based on OFDM (OFDM–M) [1]; 2) sub-band beamforming and channel estimation to achieve massive path gains by exploiting multiple antenna arrays [2]; and 3) sub-band pre-distortion for peak-to-average-power-ratio (PAPR) reduction [3] to significantly decrease the PAPR and communication errors in OFDM-IM by supporting a linear behavior of the power amplifier in the modem. The performance of the proposed framework is evaluated against the state-of-the-art QPSK, OFDM-IM [1] and QPSK-spatiotemporal QPSK-ST [2] schemes. The results show that our framework reduces the bit error rate (BER), mean square error (MSE) and PAPR compared to the baselines by approximately 6–13dB, 8–13dB, and 50%, respectively.**

I. Introduction

International Mobile Telecommunication (IMT) has set ambitious goals for year 2020 and beyond, called IMT-2020, and announced its use-cases, such as enhanced mobile broadband (eMBB), massive machine type communication (mMTC) and ultra-reliable low latency communication (URLLC) [4]. To achieve these goals, robust communication between a user equipment (UE) and the base station (eNodeB) is required. Although key technologies for 5G have been studied separately, relatively little work has been done to explore an overarching framework that seamlessly integrates them to significantly enhance the overall performance by creating synergy. To bridge this gap, we design robust wireless communication framework by leveraging advanced 5G techniques: 1) OFDM-IM [1]; 2) sub-band beamforming and channel estimation [2] and; 3) PAPR reduction [3].

First, we apply the OFDM-IM technology [1] to significantly reduce the computational cost for inverse fast Fourier transform (IFFT) and fast Fourier transform (FFT) at a UE modem and base station, respectively. In a conventional OFDM-based modem, IFFT/FFT is the most computationally expensive operation [5], because it is designed to modulate data for full size IFFT/FFT regardless of the number of active bit streams that actually deliver data. If there are fewer data, it pads dummy data bits for full IFFT/FFT operations, wasting computational resources and energy. To address this problem, we apply a novel OFDM-IM technique [1] that can dynamically adjust the number of parallel IFFT/FFT operations considering the number of incoming bit streams.

Second, we extend an effective OFDM-IM scheme [1] by applying the PAPR reduction method presented in [3] to avoid signal degradation. PAPR reduction for OFDM has gained significant attention for decades; however, much less attention has been paid to PAPR reduction for OFDM-IM. Popular PAPR reduction techniques, such as peak insertion, clipping, windowing, scrambling, block coding, and selective mapping, are mainly optimized for large amounts of data to minimize the PAPR affect [6, 7, 8, 9]. In case of mMTC and URLLC, the OFDM-IM usually deals with small amounts of data. Hence, we need an efficient PAPR technique that focuses on normalizing the power amplifier rather than tuning OFDM symbols. In this paper, we apply a novel sub-band pre-distortion PAPR reduction technique [3], which normalizes the power level of the power amplifier in the digital-to-analog-converter (DAC), for robust communication via OFDM-IM.

Further, our framework supports beamforming and channel estimation to ensure a reliable communication in 5G, to support mMTC and eMBB use cases of IMT-2020. The channel noise, fading, multi-path effects, and delay are the main challenges in 5G and mmWave communication [10]. A plenty of work has been done to address these challenges for OFDM via beamforming and channel estimation [10, 11, 12, 13]. To the best of our knowledge, however, beamforming for OFDM-IM has not been investigated yet. Sridhar et al [2] presented a novel spatiotemporal MIMO beamforming method with channel estimation to estimate the delay, direction of arrival (DoA), velocity and fading coefficients of the desired signal path. By leveraging it to enhance OFDM-IM, we significantly decrease the BER and MSE of the system.

The performance of the proposed framework is thoroughly evaluated against the existing QPSK, OFDM-IM [1] and QPSK spatiotemporal (QPSK-ST) [2] schemes. Our framework reduces the BER, MSE and PAPR compared to the baselines by approximately 6–12dB, 8–13dB, and 50%, respectively. By taking a holistic approach, we significantly improve BER, MSE, and PAPR compared to the advanced OFDM-IM [1] and QPSK-ST [2] schemes as well as the generic QPSK technique.

The rest of this paper is organized as follows. Section II discusses the proposed system framework followed by performance evaluation in section III. The paper is concluded in Section IV.

II. Robust Communication Framework

In this section, an overview of our proposed framework is given. Further, OFDM-IM, PAPR reduction, and beamforming and channel estimation are discussed.

A. System Overview

In Figure 1, the overall structure of our framework for efficient downlink communication from a base station to UEs is depicted. Our framework executes the following steps.

1) Data streams may come from one or more source to the transmitter, i.e., the base station. To distinguish them from each other, we multiply each of them with a unique pseudo-noise (PN) code. The bit splitter in Figure 1 divides these data streams into a small number of groups of a fixed size.
2) The index selector block chooses active subcarriers only.
3) The OFDM-IM modulator block modulates the active subcarriers selected by the index selector block using the mapping table stored in the corresponding mappers. Subsequently, it applies IFFT to the streams and adds a cyclic prefix (CP) to each stream to generate a subblock of symbols, similar to OFDM.
4) The PAPR reduction block pre-distorts the modulated frames in such a way that the net effect of PA becomes linear. To support beamforming, it multiplies symbols with the channel state information (CSI) matrix received from the UE. Next, it applies DAC to these streams to transmit them using an array of N_{Tx} antennas.
5) At a receiver (i.e., a UE), ADC is performed to the signal received through the antenna array with N_{Rx} antennas and then channel estimation is applied to estimate the delay, velocity, DoA and channel coefficients. In this way, the receiver estimates the transmitted signal.
6) The OFDM-IM demodulator leverages the maximum likelyhood detector to predict and cancel potential noise in the transmitted symbol estimated by the channel estimator. Next, the OFDM-IM demodulator demaps the symbol using the mapping table stored on the receiver side, applies FFT, and removes the CP. After this step, the original data stream is recovered if it is transmitted and received with no error.

B. Index Modulation

The main advantage of the MIMO OFDM-IM technique [1] over OFDM is that it selects and maps only the active subcarriers out of the incoming bit streams and applies IFFT/FFT to them to avoid unnecessary computations for any inactive subcarriers. When i different bit streams arrive at the modem on the transmitter side from one or more sources as shown in Figure 1, each of these data streams is multiplied with a unique PN code to distinguish it from the others. (The PN code also aids in beamforming which is discussed in Section II-D.) The entire PN coded active data streams, $(S_1, ..., S_i)$, goes through the bit-splitter in Figure 1, which divides the incoming bits into g groups. Notably, we do not add dummy values unlike the standard OFDM. Given that, we have $g = d/p$ groups, since there are total p bits per group.

Bits	Indices	Subblock
[0 0]	{1,2}	$[s_1\ s_2\ 0\ 0]$
[0 1]	{2,3}	$[0\ s_1\ s_2\ 0]$
[1 0]	{3,4}	$[0\ 0\ s_1\ s_2]$
[1 1]	{1,4}	$[s_1\ 0\ 0\ s_2]$

TABLE I: Mapping Table for OFDM-IM

Let N and n represent the total number of subcarriers and the total number of sub-blocks in each subcarrier in the OFDM-IM modulator, respectively. Each bit stream is transmitted using one sub-block of a subcarrier. To place bits in a sub-block, the OFDM-IM modulator uses the symbol table as shown in Table I that modulates two bits at a time. As a simple example, 00 bits are placed in the first and second place in the subblock according to the indexes in the second column in Table I. After that, they are modulated by the OFDM-IM unit that produces symbols. Next, IFFT is performed and a CP is added, similar to conventional OFDM.

C. PAPR Reduction

A high PAPR is one of the major drawbacks of a multi-carrier MIMO-OFDM system compared to a single carrier system, since it may decrease the spectrum and power efficiency, potentially increasing the BER and MSE. In this paper, we apply an efficient PAPR reduction method [3] to address this issue.

Let S_i denote the number of bit streams entering the OFDM-IM module in Figure 1, the bandwidth B of the downlink, the frequency of a sub-band that carries a sub-block, and the time duration of a single frame, respectively. A key operation in PAPR reduction is shifting each frame by Δt at time t. Since we have already applied IFFT in the OFDM-IM module, each stream S_i is transformed to the frequency domain. Thus, we time-shift the stream in the frequency domain, $\mathbb{S}_i$, as follows:

$$S_i\left(t+\Delta t\right) \equiv \left[\mathbb{S}_i\ e^{j2\pi B(t+\Delta t)}\right] \tag{1}$$

After this, we up-convert j, if j is not higher than the pre-defined intermediate frequency f_i:

$$j_{up} = \begin{cases} j \times f_i & \text{if } j \leq f_i \\ j & \text{otherwise} \end{cases} \tag{2}$$

Subsequently, j_{up} is used to create a frame.

Finally, all frames are combined in the binary search tree with depth $log_2 N$. By iteratively adding all the sub-frames pre-distorted as discussed above in the binary tree, we generate a linear amplitude for each stream for power amplification. Next, the base station performs DAC and transmits the signal of each bit stream to the UE that requested the data in the direction it received the CSI together with the data request from the UE via beamforming.(A description of beamforming is given in Subsection II-D.)

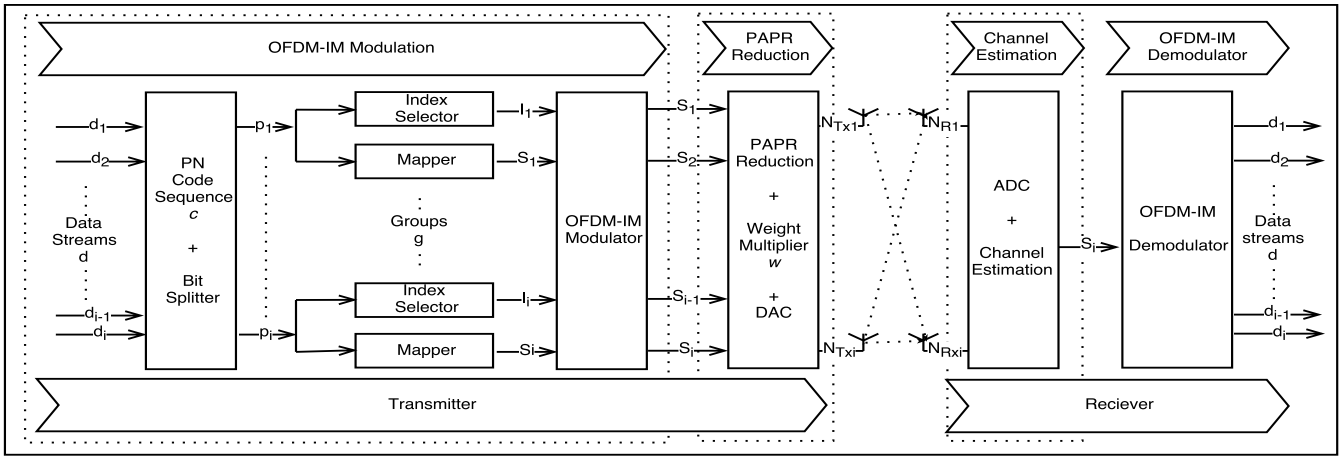

Fig. 1: Proposed End-to-End Framework

On the other hand, the receiver needs to detect the active bit streams sent from the base station to itself and the corresponding symbols. The same mapping table used in the base station is deployed at the receivers (UEs) to de-map and extract the symbols. Each receiver uses the mapping table and maximum likelihood detector to detect the locations of the symbols in the received frame.

D. Beamforming and Channel Estimation

In this paper, we apply beamforming technique to provide a directional radiation pattern by changing either the amplitude or phase of the signal in the desired direction towards UE. Also, beamforming requires the receiver to perform channel estimation to find the DoA, velocity, delay and noise coefficients of the received signal to ensure the reliable decoding of the signal. Although beamforming and channel estimation have been extensively studied in the past decade, we apply an advanced technique [2], which can provide up to 15dB improvement in terms of BER over traditional MIMO systems and is scalable up to a 500 antenna array.

1) Beamforming: The base station needs to transmit a signal to one or more UE. For reliable communication, it applies beamforming towards individual UEs as discussed before. In our framework, a UE needs to send a CSI matrix w to the base station before beginning a transmission, similar to LTE. The base station transmits the signal that has an embedded unique PN code for each UE. Further, the CSI matrix w received from the UE is concatenated at the end of the signal. The receiver listens to the direction in which it initially sent the CSI and searches for the signal that has the corresponding PN code and w.

2) Channel Estimation: In multicarrier MIMO-OFDM system, a receiver has multiple receiving antennas (N_{rx} antennas) that try to estimate the transmitted signals. An individual antenna scans for the signal with the unique PN sequence code c and w for the corresponding UE. Also, the channel estimator extracts the delay, velocity, DoA and channel fading coefficients from each antenna to extract the desired signal coming from the N_{Tx} transmitting antennas by filtering noise out. A signal is often transmitted through multiple different paths in the air and is affected by noise. Thus, we jointly estimate the delay and velocity of each path and then derive the DoA, similar to [2]. Once we have finished estimating the delay, velocity and DoA of the signal received through multiple paths, the UE combines them to find the channel coefficients using the maximum likelihood method. Finally, the OFDM-IM demodulator detects the symbols using the mapping table as discussed in Subsection II-B. The remaining steps are exactly a reverse process to that of OFDM-IM discussed in Subsection II-B.

III. Performance Evaluation

In MATLAB, the performance of the proposed framework is evaluated and compared against three state-of-the-art baselines: 1) the QPSK modulation scheme, 2) the OFDM-IM method [1] and 3) the channel estimation technique [2]. In this section, they are called QPSK, OFDM-IM and QPSK-ST, respectively. All the baselines and our approach are evaluated for four antenna array configurations: 2x2, 4x4, 6x6 and 8x8 ($N_{Tx} \times N_{Rx}$). In this paper, they are evaluated in terms of BER, MSE and PAPR. The BER and MSE are commonly used to ensure the reliability of a communication system. The BER measures the error rate of the bits received over a communication channel. The MSE is the average of the squared difference between the estimated and measured errors. The BER and MSE are largely affected by several factors, such as noise, synchronization error, phase offset, fading, delay, velocity and DoA. Each performance result presented in this paper is the mean of 1000 Monte Carlo simulations.

	2x2	**4x4**	**6x6**	**8x8**
QPSK	12dB	10dB	10dB	10dB
OFDM-IM	6dB	8dB	8dB	8dB
QPSK-ST	12dB	12dB	12dB	13dB

TABLE II: BER improvement over the baselines

Figure 2 shows the BER of the proposed framework and the three baselines. Table II summarizes the average

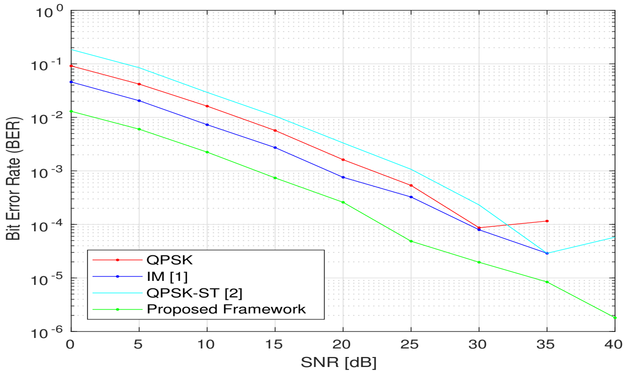

(a) BER for 2*2 Antenna Array

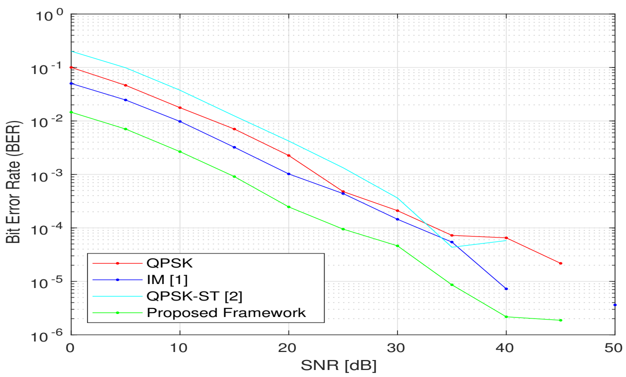

(b) BER for 4*4 Antenna Array

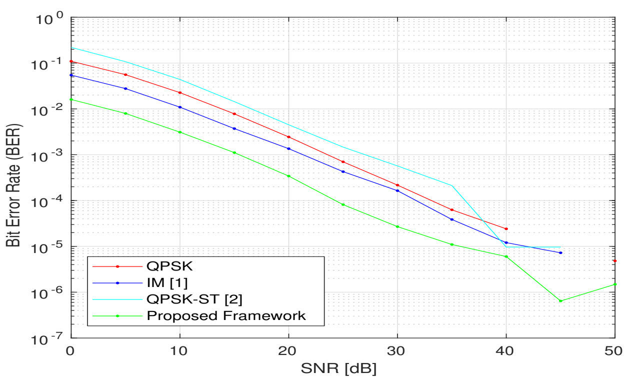

(c) BER for 6*6 Antenna Array

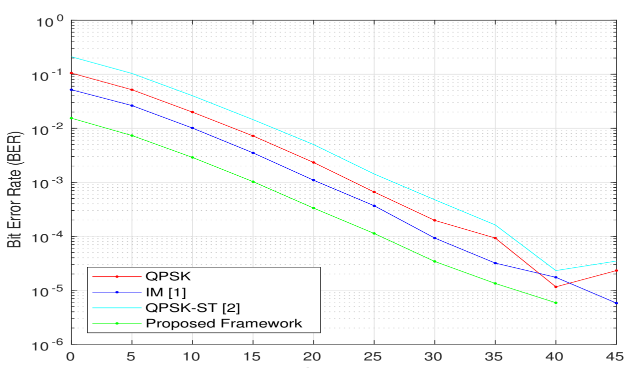

(d) BER for 8*8 Antenna Array

Fig. 2: BER Analysis Results

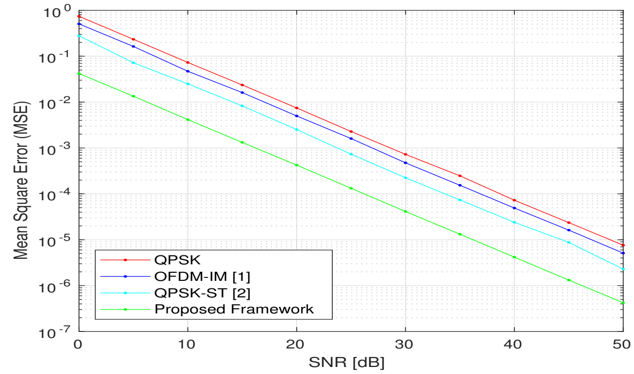

(a) MSE for 2*2 Antenna Array

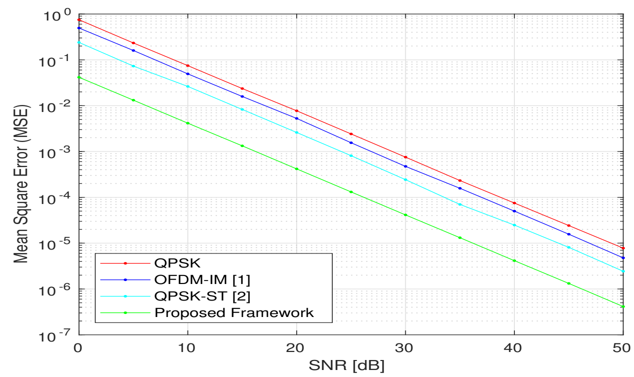

(b) MSE for 4*4 Antenna Array

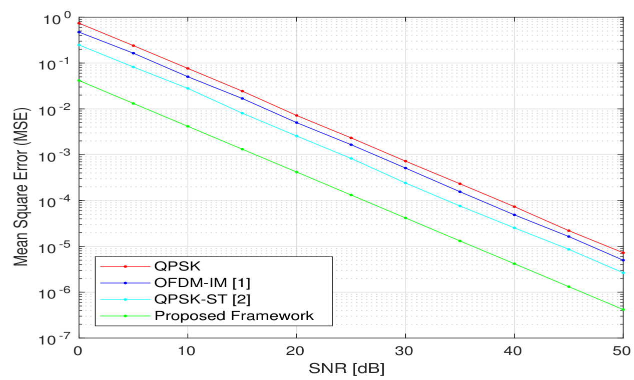

(c) MSE for 6*6 Antenna Array

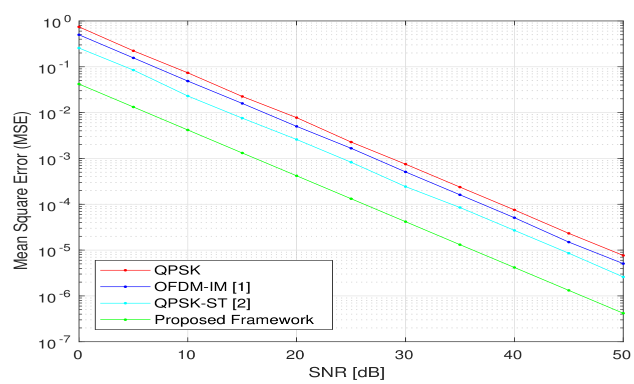

(d) MSE for 8*8 Antenna Array

Fig. 3: MSE Analysis Results

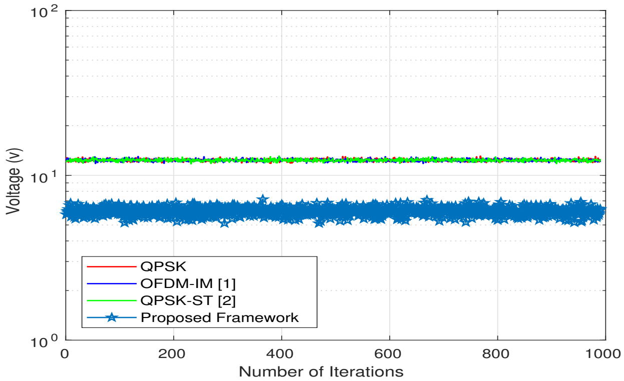

(a) PAPR for 2*2 Antenna Array

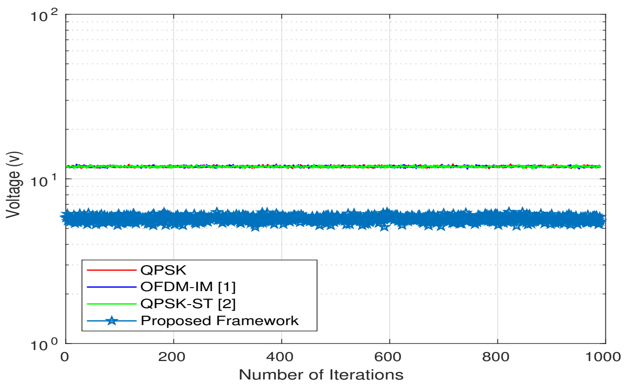

(b) PAPR for 4*4 Antenna Array

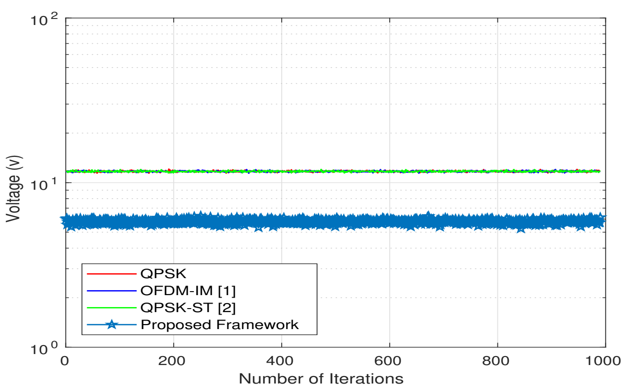

(c) PAPR for 6*6 Antenna Array

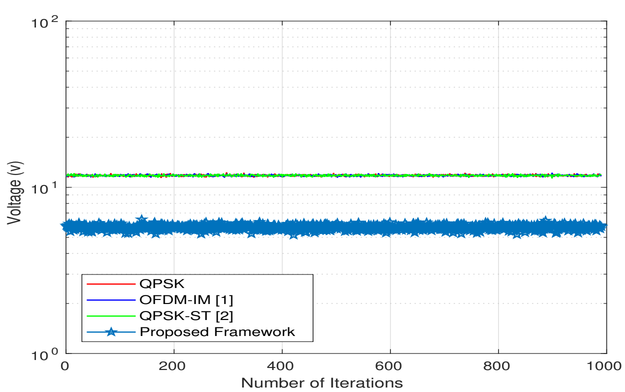

(d) PAPR for 8*8 Antenna Array

Fig. 4: PAPR Analysis Results

	2x2	**4x4**	**6x6**	**8x8**
QPSK	13dB	13dB	13dB	12dB
OFDM-IM	11dB	11dB	11dB	10dB
QPSK-ST	8dB	8dB	8dB	8dB

TABLE III: MSE improvement over the baselines

BER reduction of our approach over the baselines for each tested antenna configuration. From them, we observe that our approach significantly decreases the BER; it improves BER over QPSK, OFDM-IM and QPSK-ST by up to 12dB, 8dB and 13dB, respectively. Figure 3 plots the MSE of all the tested approaches. Also, Table III summarizes the average MSE enhancement of our approach over the baselines for each tested antenna configuration. Based on these results, we observe that our framework decreases the MSE over QPSK, OFDM-IM and QPSK-ST by up to 13dB, 11dB and 8dB, respectively.

In addition, we measure the PAPR of all the tested approaches. This is important, because multicarrier systems generally have a higher PAPR than single carrier systems do. A high PAPR may degrade the overall system performance by decreasing the signal-to-quantization noise ratio (SQNR) due to the reduced efficiency of ADC and DAC. As shown in Figure 4, our approach reduces the PAPR by more than 50% (approximately 6V) for all the antenna configurations compared to QPSK, OFDM-IM and QPSK-ST.

Overall, our holistic approach significantly reduces the BER, MSE and PAPR over not only QPSK but also advanced OFDM-IM [1] and QPSK-ST [2]. This is because, in the proposed communication system, the index modulation considering the number of active bit streams, sub-band beamforming and channel estimation to achieve massive path gains by exploiting multiple antenna array [2], and peak-to-average-power-ratio (PAPR) reduction schemes usually investigated separately cooperate with each other for robust communication and PAPR reduction.

IV. Conclusion

The upcoming 5G system requires robust communication. Although key techniques for 5G communication have been explored separately, relatively little work has been done to explore their potential cooperation for performance optimization. To address this problem, we propose a systematic approach for robust 5G communication based on MIMO OFDM by leveraging index modulation for OFDM [1], sub-band beamforming and channel estimation [2], and sub-band pre-distortion for PAPR reduction [3]. In addition to seamlessly integrating them, we apply beamforming and channel estimation to OFDM-IM, which has not been attempted before to our knowledge. The performance of the proposed framework is evaluated against the state-of-the-art QPSK, OFDM-IM [1] and QPSK-ST [2] schemes. The results show that our framework significantly reduces the BER, MSE and PAPR compared to the baselines by approximately 6–13dB, 8–13dB, and 50%, respectively. In the future, we will continue to investigate how to enhance the robustness and reduce the PAPR further.

ACKNOWLEDGMENT

This work was supported, in part, by NSF grant CNS-1526932.

REFERENCES

[1] Ertugrul Basar. “Index modulation techniques for 5G wireless networks”. In: *IEEE Communications Magazine*. 2016.

[2] Vidhya Sridhar, Thibaud Gabillard, and Athanassios Manikas. “Spatiotemporal-MIMO Channel Estimator and Beamformer for 5G”. In: *IEEE Transactions on Wireless Communications*. 2016.

[3] Feng Lu et al. “Sub-Band Pre-Distortion for PAPR Reduction in Spectral Efficient 5G Mobile Fronthaul”. In: *IEEE Photonics Technology Letters*. 2017.

[4] ITU. “Recommendation ITU-R M.2083-0 Policy on Intellectual Property Right (IPR) Series of ITU-R Recommendations”. In: ().

[5] Taewon Hwang et al. “OFDM and Its Wireless Applications: A Survey”. In: *IEEE Transactions on Vehicular Technology*. 2009.

[6] C Matrakidis. “Multicarrier Transmission Peak-to-average Power Reduction Using Simple Block Code - Electronics Letters”. In: vol. 34. 10. 1998, pp. 953–954.

[7] Xiaojing Huang, Y. Jay Guo, and John D. Bunton. “A hybrid adaptive antenna array”. In: *IEEE Transactions on Wireless Communications*. 2010.

[8] Ahmed Alkhateeb et al. “Channel Estimation and Hybrid Precoding for Millimeter Wave Cellular Systems”. In: *IEEE Journal of Selected Topics in Signal Processing*. 2014.

[9] Omar El Ayach et al. “Spatially Sparse Precoding in Millimeter Wave MIMO Systems”. In: *IEEE Transactions on Wireless Communications*. 2014.

[10] Wonil Roh et al. “Millimeter-wave beamforming as an enabling technology for 5G cellular communications: theoretical feasibility and prototype results”. In: *IEEE Communications Magazine*. Vol. 52. 2. Feb. 2014, pp. 106–113.

[11] Maliheh Soleimani et al. “Hybrid Beamforming and DFT-Based Channel Estimation for Millimeter Wave MIMO Systems”. In: 2017. ISBN: 9781538635315.

[12] Min Li et al. “Beamforming for Dual-Hop MIMO AF Relay Networks with Channel Estimation Error and Feedback Delay”. In: *IEEE Access*. Vol. 5. 2017, pp. 21840–21851.

[13] Devendra Singh Gurjar et al. “Beamforming in Traffic-Aware Two-Way Relay Systems With Channel Estimation Error and Feedback Delay”. In: *IEEE Transactions on Vehicular Technology*. Vol. 66. 2017, pp. 8807–8820.